

**TexAQS-II Meteorological Model Performance Evaluation Framework
(Task A2)**

John Nielsen-Gammon, James Tobin, and Tatiana Erukhimova

The Center for Atmospheric Chemistry and the Environment

Texas A&M University

August, 2005

Revised December, 2005

Purpose

The purpose of this report is to describe the real-time MM5 model configuration during summer 2005, the procedures for the verification of the MM5 numerical weather forecasts being generated by Texas A&M University for air quality forecasting and other decision making purposes during the Second Texas Air Quality Study (TexAQS-II), and a preliminary evaluation of model performance.

Note: The preparation of this report is based on work supported by the State of Texas through a Contract from the Houston Advanced Research Center, Texas Environmental Research Consortium and the Texas Commission on Environmental Quality.

Contact Information:

John W. Nielsen-Gammon
Center for Atmospheric Chemistry and the Environment
Texas A&M University
3150 TAMUS
College Station, TX 77843-3150
n-g@tamu.edu
979-862-2248
979-862-4466 (f)

PART 1: MODEL CONFIGURATION

Grid Setup

We are using the MM5 numerical model, version 3. This model is selected over the WRF model because of its successful history in support of air quality simulations in Texas and because the anticipated GOES satellite data assimilation tool from the University of Alabama at Huntsville (UAH) is designed for MM5.

The projection and orientation of the model domains are constrained by the projection and orientation of the emissions inventory used by the Texas Commission on Environmental Quality (TCEQ) to be a Lambert projection with true north oriented along 100 W.

The outer domain in our TexAQS-2000 simulations had a grid spacing of 108 km. In view of current processor speeds, such a large grid spacing is unnecessary. Furthermore, it is desirable to resolve continent-scale transport at higher resolution than 108 km. Thus, our outer grid is 36 km. The grid is defined to extend sufficiently far south to include the areas of southern Mexico and Guatemala that are often sources of smoke for Texas in the springtime. An intermediate grid has 12 km grid spacing, and the finest grid has 4 km grid spacing.

The minimum resolution of the model is driven by previous experience with meteorological modeling in the Houston area, which suggests that a 4 km grid spacing is able to resolve the sea breeze without adversely resolving turbulent PBL structures. Because the state of Texas is interested in regional haze as well as ozone pollution, we have established a 4 km grid that includes almost the entire state of Texas (except for El Paso) as well as most of Oklahoma, Arkansas, and Louisiana. The eastern border of the grid was constrained to include the 4 km modeling domain from TexAQS-2000 modeling efforts. With additional computer power, the entire state of Texas can be simulated at 4 km grid spacing.

The large 4 km grid is not an issue for photochemical modeling because high-resolution photochemical models can easily be run on a subset of the 4 km grid, even with multiple overlapping or non-overlapping nests. The common projection guarantees that the 4 km

modeling by TCEQ and the University of Houston (UH) consists of collocated grid points within the large 4 km grid.

Here is an excerpt from terrain.deck that defines the horizontal grid setup. Note that only the first three nests are used for the real-time modeling.

```

&MAPBG
PHIC = 40.0, ; CENTRAL LATITUDE (minus for southern hemesphere)
XLONC = -100.0, ; CENTRAL LONGITUDE (minus for western hemesphere)
IEXP = .F., ; .T. EXPANDED COARSE DOMAIN, .F. NOT EXPANDED.
; USEFUL IF RUNNING RAWINS/little_r
AEXP = 360., ; APPROX EXPANSION (KM)
IPROJ = 'LAMCON', ; LAMBERT-CONFORMAL MAP PROJECTION
;IPROJ = 'POLSTR', ; POLAR STEREOGRAPHIC MAP PROJECTION
;IPROJ = 'MERCAT', ; MERCATOR MAP PROJECTION
&END
&DOMAINS
;
MAXNES = 5, ; NUMBER OF DOMAINS TO PROCESS
NESTIX = 163, 136, 316, 82, 160, 221, ; GRID DIMENSIONS IN Y DIRECTION
NESTJX = 185, 175, 343, 61, 91, 221, ; GRID DIMENSIONS IN X DIRECTION
DIS = 36., 12., 4., 12., 4., 1.0, ; GRID DISTANCE
NUMNC = 1, 1, 2, 1, 4, 5, ; MOTHER DOMAIN ID
NESTI = 1, 33, 16, 71, 15, 50, ; LOWER LEFT I OF NEST IN MOTHER DOMAIN
NESTJ = 1, 73, 18, 140, 15, 50, ; LOWER LEFT J OF NEST IN MOTHER DOMAIN
RID = 1.5, 1.5, 1.5, 1.5, 1.5, 2.3, ; RADIUS OF INFLUENCE IN GRID UNITS
(IFANAL=T)
NTYPE = 3, 4, 6, 4, 5, 6, ; INPUT DATA RESOLUTION
NSTTYP= 1, 2, 2, 1, 2, 1, ; 1 -- ONE WAY NEST, 2 -- TWO WAY NEST
&END
&OPTN
IFTER = .TRUE., ; .T.-- TERRAIN, .F.-- PLOT DOMAIN MAPS ONLY
DATASW = .T., ; .T. user specify terrain and landuse resolution (ntype)
; .F. terrain program choose the data resolution
IFANAL = .F., ; .T.-- OBJECTIVE ANALYSIS, .F.-- INTERPOLATION
ISMTHTR = 2, ; 1: 1-2-1 smoother, 2: two pass smoother/desmoother
IFEZFUG = .F., ; .T. USE NCAR GRAPHICS EZMAP WATER BODY INFO TO FUDGE THE LAND
USE
; .F. USE LANDWATER MASK DATA
IFTFUG = .F., ; .T. DON'T DO EZFUDGE WITHIN THE USER-SPECIFIED
; LAT/LON BOXES, need to define namelist fudget
IFFUDG = .F., ; .T. POINT-BY-POINT FUDGING OF LANDUSE,
; need to define namelist fudge
IPRNTD = .F., ; PRINT OUT LAT. AND LON. ON THE MESH
IPRHTH = .F., ; PRINT OUT ALL PROCESSING FIELDS ON THE MESH
IPRINT = 0, ; = 1: A LOT MORE PRINT OUTPUT IN terrain.print.out
FIN = 100., 100., 100., 100., 100., 100., ; CONTOUR INTERVAL (meter) FOR TERRAIN
HEIGHT PLOT
;TRUELAT1 = 91., ; TRUE LATITUDE 1
;TRUELAT2 = 91., ; TRUE LATITUDE 2, use this if IPROJ='LAMCON'
IFILL = .TRUE., ; .TRUE. --- color filled plots
LSM DATA = .TRUE., ; .TRUE. --- Create the data for LSM
VEGTYPE = 1, ; LANDUSE DATA TYPE: =0: old 13 cat; =1: 24 cat USGS; =2: 16 cat
Sib
VS PLOT = .TRUE., ; .TRUE. --- plot Vege., Soil, Vege. Frc. percentages.
IEXTRA = .FALSE., ; .TRUE. --- Create extra data for Pleim-Xiu LSM
&END

```

A graphical depiction of the horizontal domains is shown in Fig. 1.

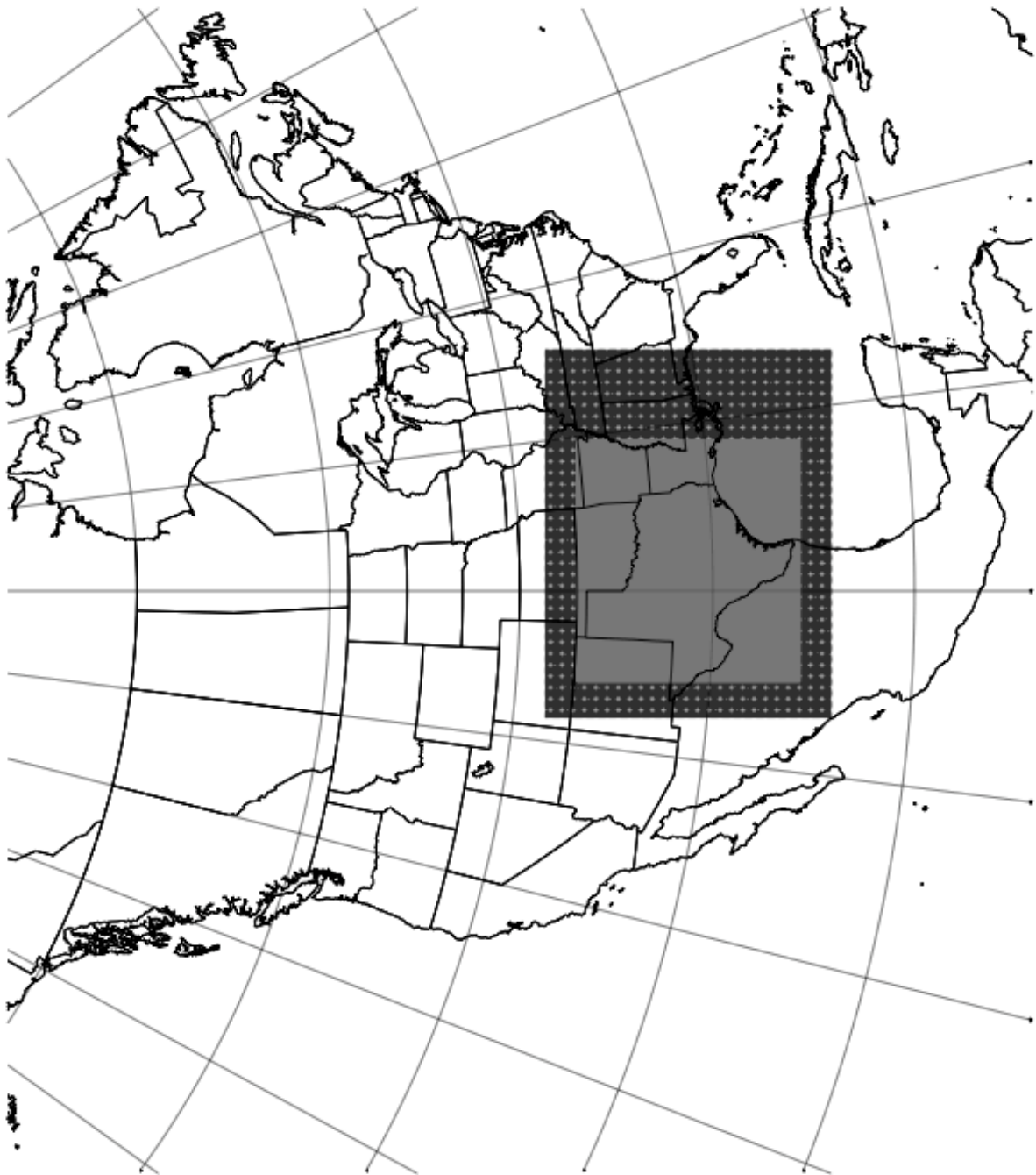


Figure 1: Outermost 36 km domain, with locations of 12 km domain (black) and 4 km domain (gray).

The vertical grid spacing is identical to that used in TCEQ’s TexAQS 2000 Houston ozone episode modeling. Tests were conducted to determine the sensitivity of the model results to the vertical grid spacing. We found that the 43 layer model, as used for TexAQS 2000, was adequate, and that additional vertical layers did not have a significant impact. A description of these experiments is provided in an attached report. Based on these results, the vertical grid configuration was unchanged from that used by TCEQ and UH.

Here is an excerpt from `interp.f’s namelist.input`, showing the vertical grid configuration and other configuration information:

```
&record2
  sigma_f_bu      = 1.000,0.996,0.990,0.980,0.970,0.960,0.950,      ! full sigma, bottom-
up,
                  0.940,0.930,0.920,0.910,0.895,0.880,      ! start with 1.0, end
                  0.865,0.850,0.825,0.800,0.775,0.750,      ! with 0.0
                  0.720,0.690,0.660,0.630,0.600,0.570,
                  0.540,0.510,0.475,0.440,0.405,0.370,
                  0.330,0.290,0.250,0.210,0.175,0.145,
                  0.115,0.090,0.065,0.045,0.025,0.010,
                  0.000
  ptop            = 10000      ! top pressure if need to be
redefined
  isfc            = 0 /      ! # sigma levels to spread
                        ! surface information

&record3
  p0              = 101300     ! base state sea-level pres (Pa)
  tlp             = 45.        ! base state lapse rate d(T)/d(ln
P)
  ts0            = 304.        ! base state sea-level temp (K)
  tiso           = 200./      ! base state isothermal
stratospheric temp (K)
```

Model Physics

Major model physics options are as follows.

Cloud Microphysics: The “simple ice” scheme is used. This scheme is a relatively fast scheme that has been used in most, if not all, Texas air quality modeling. It tracks two hydrometeor species (cloud and precipitation), and is appropriate for simulations that do not require highly accurate representation of precipitation processes.

Cumulus Parameterization: The “Grell” scheme is used on the 36 km and 12 km grids, and no scheme is used on the 4 km grid. This scheme is a fast hybrid scheme, suitable for high-resolution modeling, and was used in previous modeling for TexAQS 2000. Shallow convection is activated on all grids.

Vertical Mixing: The “MRF” scheme is used. This scheme, also used for Texas A&M’s simulations for TexAQS 2000, was chosen because it is the only scheme presently compatible with GOES satellite assimilation. Even though no such assimilation was performed during 2005, the model was configured so as to be ready for assimilation.

Land Surface: The multi-layer soil model is used, again for compatibility with GOES satellite assimilation. Aside from the size of the inner domain, this is the primary difference with the real-time UH runs, which utilize the NOAA land surface model with enhanced land use/land cover for eastern Texas.

Initial and Boundary Conditions

The model is driven by the 32-km Eta gridded output, the only high-resolution output that covers our outer model domain. The Eta analysis is used as the initial condition for the model, with no additional assimilation of local data during 2005. The boundary conditions are taken from the Eta model forecast initialized from the same analysis. The analyses are compatible with the analyses used for the TexAQS 2000 modeling, known as EDAS analyses, with NCEP having made incremental changes to their analysis scheme since 2000.

Following acquisition of data directly from NCEP from the 00Z model run cycle, model execution begins around 10:30 PM CDT. The model finishes about 8:00 AM. The model run was initially designed to last 56 hours, to forecast information for two days and two nights. During the Northeast Texas Plume Study (NETPS), the mission scientists needed forecast information for three days, so the duration of the forecast cycle was extended to 72 hours in early August.

Differences from Previous Modeling

The real-time forecast model runs will be most similar to the modeling used for the Houston-Galveston SIP work. Primary differences include the larger inner domain, which for the area covered by the original inner domain will improve simulation quality near the boundaries, and land surface representation. A variety of approaches have been tried in Texas for land surface simulations, including land surface modeling, soil moisture specification, and

satellite data assimilation. The real-time modeling uses none of these approaches. In that respect it is most similar to the soil moisture specification approach, except that the default soil moisture values are utilized. Significant differences would be expected between the surface meteorological conditions, especially temperature and moisture, in the real-time runs at Texas A&M compared to those at UH. While one might expect that a more sophisticated land surface treatment, such as is used by UH, will yield better results, there is value in having an alternative representation at Texas A&M so that a variety of forecast scenarios are simulated and the dependence of a given day's forecast on land surface conditions can be ascertained.

PART 2: PERFORMANCE EVALUATION FRAMEWORK

Introduction

Forecast verification involves studying the relationship between one or more forecasts and their corresponding observations. There are four basic ways in which this can be done. First, a single forecast can be compared with a single observation. This is the simplest form of verification and the one that most likely comes to mind when one thinks of forecast verification. Being the simplest, however, this is also the least useful and will not be relied upon heavily, if at all, during this study. Verifications can also be performed using a set of multiple forecasts for different locations at the same time, or for the same location at different times. Finally, a set consisting of multiple forecasts for different locations and different times may be evaluated.

Over 50 years ago, Brier and Allen categorized the various reasons for forecast verification into three types: administrative purposes, scientific purposes and economic purposes (Jolliffe and Stephenson 2003). Murphy (1993) notes that the criteria for a “good” forecast may vary based on the objectives of the forecast and the decision-making problems to which it is applied. During TexAQS-II model forecasts will be verified for two of these three purposes. Forecasts will be evaluated for administrative purposes as a tool for making air quality regulatory decisions. Forecasts will also be verified in an attempt to scientifically validate the model, particularly in reference to sea breeze strength and timing, diurnal temperature and wind cycles,

and the spatial distribution of temperature errors as they pertain to errors in model land cover versus model meteorology. Descriptions for each of these verifications are provided in the following sections.

Verification Techniques

Procedures for each of the necessary verifications follow. In all cases the verifications will take place in observation space. This means that model forecasts will be interpolated to observation locations. The alternative approach, using a gridded analysis for verification, is rejected here because no suitable high-resolution analysis exists and data inhomogeneities make the creation of such an analysis subject to errors in its own right.

A. Administrative Verifications

One of the most common measures of accuracy employed in the verification of deterministic forecasts is the mean squared error (MSE), which for a set of n matched pairs of forecasts and observations is given by:

$$MSE = \frac{1}{n} \sum_{i=1}^n (f_i - x_i)^2,$$

where f_i and x_i represent the i^{th} forecast and observation, respectively. The set of forecast-observation pairs may be from multiple locations at the same time or for the same location at multiple times. Murphy (1988) demonstrates that this MSE can be decomposed into the sum of four parts, as follows:

$$MSE = (\bar{f} - \bar{x})^2 + s_f^2 + s_x^2 - 2s_{fx},$$

where the terms in this decomposition correspond to the bias, forecast variance, observation variance, and two times the covariance between forecasts and observations, from left to right.

Murphy (1988) also suggests a skill score in terms of the MSE. This skill score is:

$$SS = 1 - \frac{MSE(f, x)}{MSE(r, x)},$$

where $MSE(f,x)$ is the MSE of the actual forecast-observation pairs and $MSE(r,x)$ is the MSE of the reference forecast-observation pairs. The difference between a skill score and a measure of accuracy is that the skill score compares the model forecasts with some reference forecast, typically persistence or climatology. For the administrative verification of this model the reference forecast could be either persistence (the previous observation, or 24-hour previous observation for variables with a significant diurnal cycle), a model forecast for the same verification time from a previous model run, or climatology if a sufficient climatology exists. More precise reference forecasts will be proposed for the scientific verifications discussed in the next sections.

Fitting the predictions to the observations through least-squares linear regression can also provide useful information for an administrative verification of the model. Willmott (1982) suggests that the regression coefficients be reported, and the correlation between the observations and predictions (from the r^2 value of the regression) is also a useful measure for model verification. Fitting a model of the form:

$$f_i = a + bx_i,$$

the regression coefficients a and b can then be used to determine a fitted prediction \hat{f}_i for each observation. Using these fitted predictions, the MSE can be broken down into systematic and unsystematic components, where the systematic component of the MSE is $MSE(\hat{f}_i, x)$, the unsystematic component of the MSE is $MSE(f, \hat{f}_i)$, and the system is additive such the systematic and unsystematic component of the MSE sum to the total MSE. An experiment with this decomposition method (not shown) indicated that this method can be very sensitive to outliers if only a small number of forecast-observation pairs are used. Therefore it is not recommended that much weight be given to the results of this verification unless a large data set is used. It is still worthwhile to report the results of this verification, however, particularly the correlation (r^2 value) between forecasts and observations. This method of MSE decomposition will be relied upon more heavily in the scientific evaluation of the spatial distribution of temperature errors.

One final diagnostic measure of model performance that may be useful for administrative verification is the index of agreement (IOA). Willmott (1982) gives the equation for the IOA as:

$$IOA = 1 - \frac{\sum_{i=1}^n (f_i - x_i)^2}{\sum_{i=1}^n [|(f_i - \bar{x})| + |(x_i - \bar{x})|]}$$

The formula for this descriptive measure of model performance is similar in form to that for the MSE skill score and is bounded by 0 (no agreement between forecasts and observations) and 1 (perfect agreement between observations and forecasts). The IOA may be a good measure of model performance both at a particular time (for all points at that time) and at a particular location (for a set of forecast-observation pairs from previous times at that point).

Also, see Murphy et al. (1987) for additional suggestions of administrative verification methods, particularly those pertaining to the joint probability distribution framework for forecast verification (Murphy and Winkler 1987).

B. Sea Breeze and Diurnal Wind Variations

For the first of the scientific verifications, the MSE will once again be used as the standard measure of accuracy. In the case of verifying the sea breeze and diurnal wind variations, the MSE of both the observations and the forecasts will be decomposed. Theory suggests that the turning of the wind just above the influence of topography (or surface wind just offshore) will trace out an ellipse over a 24-hour period. The axes and orientation of this ellipse can be determined via least squares regression by fitting a model of the form

$$u = a_u + b_u t + c_u \sin\left(\frac{2\pi t}{24} + d_u\right)$$

$$v = a_v + b_v t + c_v \sin\left(\frac{2\pi t}{24} + d_v\right)$$

to one day's worth of u- and v-wind observations and forecasts at any location (surface data at buoy stations or profiler data at 100-200 meters over land). The terms in this model correspond to the bias (systematic error), synoptic (linear) changes, and diurnal (sinusoidal) changes. A ratio of the amount of MSE attributed to each source in the observations versus the forecasts can

be reported, such that values of 1 suggest a perfect match in the amount of variance explained between the forecasts and the observations. As particular measures of the model error in the sea breeze, the difference between the size and orientation of the ellipse can be reported as well as the difference in timing along the elliptical path with respect to flow heading in a particular direction (perhaps inland, or more simply due north). It is possible that a Brier-like skill score can even be calculated by taking the amount of overlapping area between the forecasted and observed ellipses, which could be considered to be centered on their station of reference.

C. Spatial and Diurnal Distribution of Temperature Errors

The techniques for evaluating the spatial distribution of temperature errors were laid in the administrative verification section in the discussion of regression. In this case the assumption is added that systematic errors (model biases) correspond to land cover errors and unsystematic errors correspond to other factors, referred to here as “meteorology”. Any ideal model with MSE decomposed in this manner would have a systematic MSE approaching zero and an unsystematic MSE approaching the total MSE. This is no exception since the systematic MSE corresponds to errors that are inherent in the model. In this case the decomposition of MSE should be performed for all points in observation space at any one time. A plot of the correlations between recent errors at each station may also be helpful by identifying regions where errors are highly correlated. This does not necessarily implicate the model or the observations, but does suggest that one or both are systematically biased since errors more than a few hours apart and attributed only to “meteorology” at any one point should be uncorrelated. A periodogram of the forecast errors at each point over a period of several days may also be pertinent to this verification.

For deducing diurnal temperature variations, the MSE is computed over an extended period as a function of time of day and decomposed into systematic and unsystematic errors. Furthermore, because model biases due to land surface processes are likely to be sensitive to particular land surface characteristics, the temperature errors at particular stations will be analyzed spatially as described in the preceding paragraph.

D. Subjective Verification

Apart from objective techniques of forecast verification, subjective verification is necessary for obtaining a complete picture of model performance in forecasts of particular phenomena or particular features of interest. Subjective verification requires intensive examination of forecast model output and comparison with observations. For that reason, a large portion of the subjective verification activities will be conducted during times of providing forecasting support for TexAQS-II field activities.

Subjective verification will focus on the following aspects of model performance: daytime wind forecasts, forecasts of the presence and absence of convection, sea breeze evolution, and low-level jet formation. Aspects such as the consistency of model forecasts, the apparent effects of initialization with large-scale models, and impacts of model configuration will be examined.

Subjective Verification

Based on experience working with the model output in preparation for and during the Southeast Texas Transport Study and the Northeast Texas Plume Study, the following aspects of model performance are noted:

1. Overall the MM5 performed very well during July and August. The model was much more valuable for forecasting guidance than operational numerical models run by national centers. This advantage is due to both the superior resolution of the MM5 runs and the ability to generate products that directly target air quality and forecasting needs.
2. During situations in which convective activity was possible, the model had a tendency to produce too much precipitation and generate too much organization into convective systems and squall lines. This tendency was not uniform; on several occasions the model underforecasted the amount of precipitation. It was necessary at times to infer what the distribution of winds would be in the absence of convection when the model forecasted convection and no convection was likely.
3. The model also had a tendency to produce much more precipitation inside the edge of the 4 km inner domain than outside the 4 km domain. This behavior suggests that the model's 36

km and 12 km convective parameterization was adjusting the simulated atmosphere to a state that was still absolutely unstable on the 4 km domain.

4. The model produced a nighttime sea breeze jet that, under large-scale light onshore wind conditions, intensified to 25-30 kt and spread inland about 200 miles. Because of the location of the sea breeze jet and the absence of strategically-placed profilers, the forecasters were initially uncertain whether this jet was real. Eventually enough events affected profiler sites in Huntsville and Cleburne that it appears that the model simulation is realistic and is essentially simulating a new phenomenon.

5. Wind forecasts for Day 2 appeared to be comparable in accuracy to forecasts for Day 1. This means that the model spinup time over the course of a day has a noticeable beneficial effect on the forecast quality despite the increased forecast range. An assimilation or model initialization scheme that is consistent with the resolution and model physics of the MM5 would have an immediate positive benefit.

6. The model seemed to be reasonably accurate with its forecasts of mixing heights and daytime wind evolution. At times, the model seemed to have a bias in North Texas in which it underestimated the southeasterly component of the wind. Otherwise the model behaved well with the timing of stagnation in the morning and the onset of easterlies or southeasterlies in the afternoon.

Timetable

Because many of the statistical techniques to be applied to MM5 verification require a large number of realizations to yield robust results, we have been archiving MM5 forecasts and observational verification information since the initiation of real-time forecasting in the spring. We will wait for additional realizations to accumulate in September before beginning an ozone-season verification study in October. This model verification phase will take a few months to complete, but will yield valuable information both for model tuning prior to next ozone season and for retrospective model runs for photochemical modeling.

Summary

1. The MSE will be used as the primary measure of accuracy in model verification.
2. The MSE skill score will be used for the administrative verification of most forecasts, using all the forecast-observation pairs in observation space on any one grid at any one time.
3. The sea-breeze and diurnal wind variation will be verified by decomposing the MSE of the observed and forecasted values during a 24-hour period using a special model form including a sinusoidal term designed to incorporate the diurnal cycle in the winds.
4. The spatial distribution of temperature errors will be examined via a decomposition of temperature forecasts as described in the administrative verification section, along with an examination of error correlation in both space and time.
5. The diurnal cycle in the temperature forecasts will be verified in a manner similar to the spatial distribution of temperature errors.
6. To assess the model, MSE, MSE skill scores, and ratios of forecasted to observed MSE will be reported. Useful plots may include periodograms or correlograms for individual stations, q-q or p-p plots for individual forecast times, and spatial plots of error correlation.
7. The MM5 performed very well overall during the summer. Some biases were noted in precipitation distribution and southeasterly winds, but the model also produced forecasts of unexpected nighttime phenomena that were subsequently verified by observations.
8. Further objective verification and improvement of the MM5 real-time forecasting system will take place in the fall and winter.

References for Part II

Jolliffe, I.T. and D.B. Stephenson, 2003: *Forecast Verification*. John Wiley & Sons Ltd., Chichester, West Sussex, England, 240 pp.

Murphy, A.H., 1988: Skill Scores Based on the Mean Square Error and Their Relationships to the Correlation Coefficient. *Mon. Wea. Rev.*, **116**, 2417-2424.

- 1993: What Is a Good Forecast? An Essay on the Nature of Goodness in Weather Forecasting. *Wea. and Forecasting*, **8**, 281-293.
- , B.G. Brown and Y.-S. Chen, 1989: Diagnostic Verification of Temperature Forecasts. *Wea. and Forecasting*, **9**, 485-501.
- and R.L. Winkler, 1987: A General Framework for Forecast Verification. *Mon. Wea. Rev.*, **115**, 1330-1338.
- Wilks, D.S., 1995: *Statistical Methods in the Atmospheric Sciences*. Academic Press, San Diego, CA, 467 pp.
- Willmott, C.J., 1982: Some Comments on the Evaluation of Model Performance. *Bull. Am. Meteorol. Soc.*, **63**, 1309-1313.

PART III: MODEL PERFORMANCE

Overview

The objective verification scheme was not yet installed and operational during Summer 2005, so we limit ourselves to subjective verification of the model, with particular focus on those aspects of the model simulations that were necessary for field support during the Southeast Texas Transport Study (SETTS) and NETPS.

The value of any forecast support tool can be measured by how much it is utilized for forecasting purposes. In that respect, the real-time modeling was highly successful. It was relied upon as the principal forecast tool for NETPS, and as forecasters gained experience with the model, that reliance only increased with time. The model forecasts, properly interpreted and converted into field operations guidance, never caused operations to take place inappropriately, nor did operations fail to take place when they should have been undertaken.

The following sections deal with the three most critical aspects of model performance with respect to field operations during 2005: the sea breeze, nighttime transport, and precipitation.

Sea Breeze Forecasts

Forecasts of the sea breeze were critical for SETTS. With balloon releases undertaken during the evening on all three days, the most important aspects of the forecast were the daytime transport from Houston and the likelihood of convection.

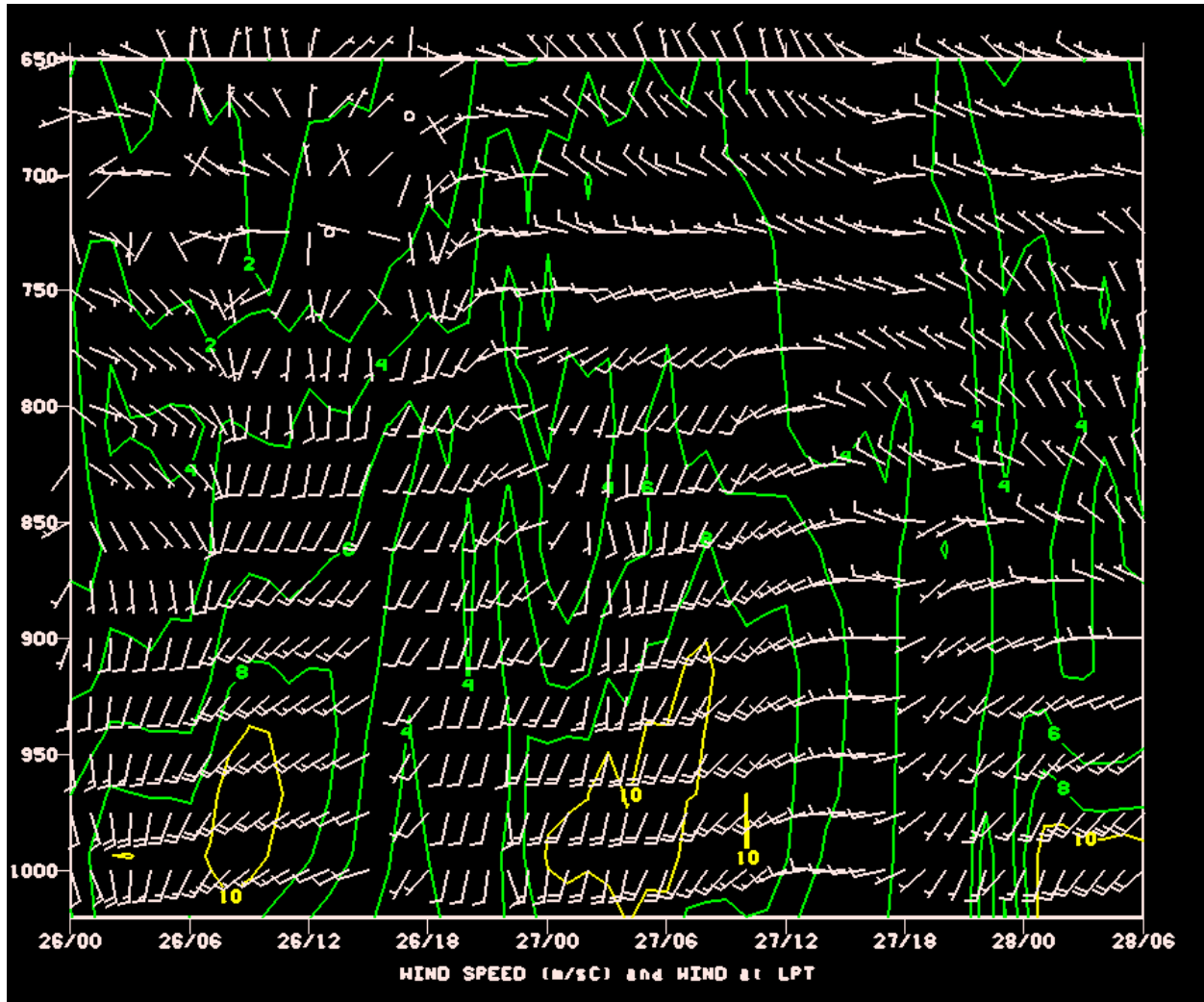


Figure 2: Time-height section of forecasted wind at the LaPorte profiler site. Wind speed is contoured in m/s. The vertical axis is pressure (mb).

The real-time model performed well in its simulation of the well-documented daily wind variation in the Houston area. The model correctly produced an elliptically-varying wind, with strongest onshore flow in the evening and weakest onshore flow during the morning. Figure 2 shows an example from during SETTS. At low levels (below 900 mb, or about 1 km AGL), the model predicted southwesterly winds approaching 10 m/s overnight, with strongest winds around 0800-0900 UTC (3:00-4:00 AM CDT). The winds were forecast to weaken throughout the morning, becoming weak, particularly at low levels, around 1700 UTC (12:00 Noon CDT). During the afternoon, light winds from the south or southeast were forecasted to rapidly strengthen after 2200 UTC (5:00 PM CDT), becoming strong from the south and veering to the southwest overnight. The strongest winds were forecasted to be confined to the layer below 900 mb, with winds relatively light and variable above 800 mb (about 2 km).

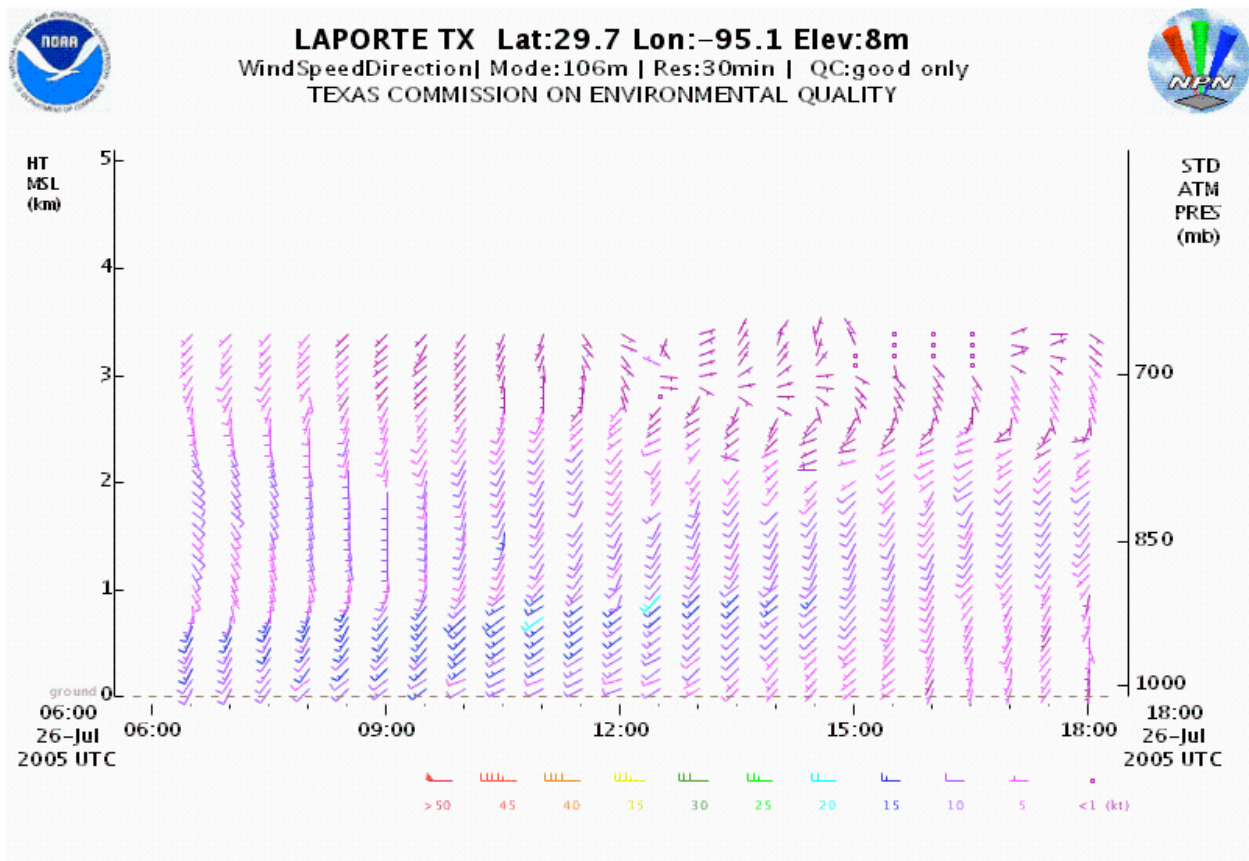


Figure 3: Observed winds at LaPorte profiler. Wind barb plotting convention is same as in Fig. 2, while wind speeds are color-coded in knots (divide by 2 to get m/s).

The actual winds at LaPorte were similar. The strongest winds overnight (Fig. 3) occurred around 0900-1000 UTC, peaking at about 10 m/s. During the morning, the wind speeds decreased, and after 1500 UTC (10:00 AM CDT), the winds changed direction from southwesterly to southerly, as forecasted by the model. During the afternoon, the lowest-level winds became southeasterly before strengthening again from the south (Fig. 4). Overnight, winds remained relatively strong and veered from south to southwest.

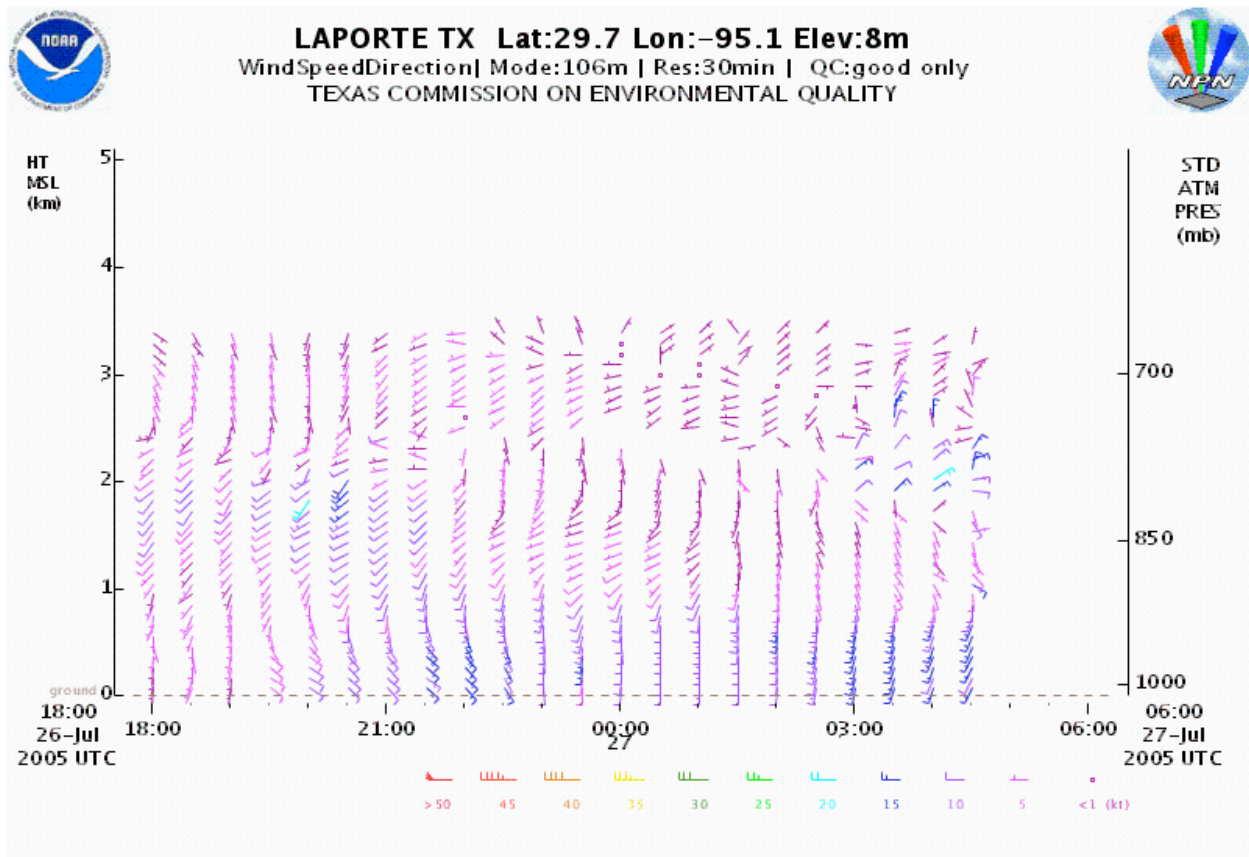


Figure 4: Observed winds at LaPorte profiler, as in Fig. 3, but for afternoon and evening of July 26, 2005.

The longer-range forecast for the second day was nearly a carbon copy of the first day (Fig. 2). Winds again were forecasted to weaken from the west (rather than from the southwest) before becoming light from the southwest during the afternoon. The actual winds (Fig. 5) developed more of a northerly wind component during the morning while weakening. This difference is consistent with the model overestimating the large-scale southerly winds during the latter portion of the period. This sort of model behavior was seen repeatedly during the field

program: the numerical model would correctly simulate the variation in winds over the course of the day, but would have increasingly large errors in the overall wind pattern as the forecast stretched out to two or three days.

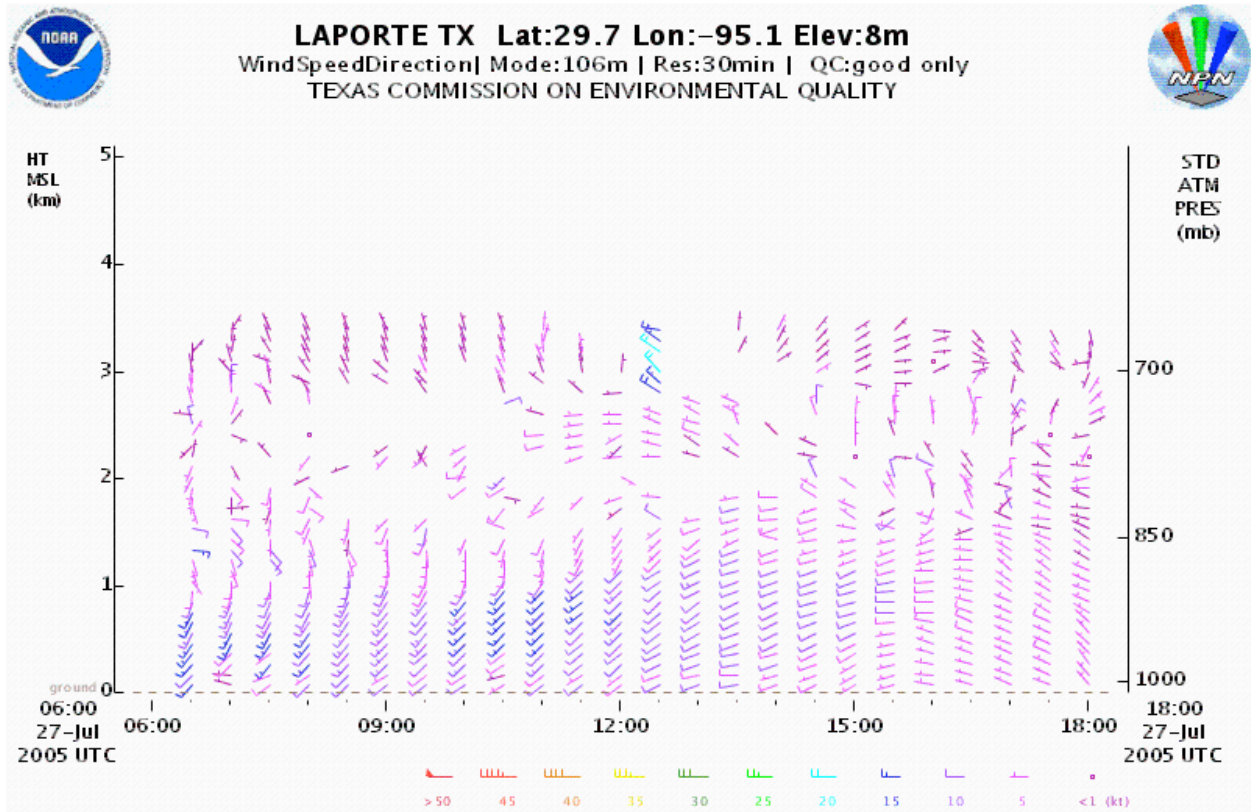


Figure 5: Observed winds at LaPorte profiler, as in Fig. 3, but for morning of July 27, 2005.

This sort of forecast error is good, in a sense, because it implies that the model captures the essential physical processes associated with the sea breeze. For application to air quality simulations, for which data assimilation would be performed, the model would utilize the observations for constraining the overall evolution of the wind field, but the observations would not be needed to “force” the model to reproduce a physical process such as the sea breeze that it would otherwise be unable to replicate. In this case, the model does replicate the sea breeze.

Despite its fidelity with the sea breeze, the larger-scale wind errors inherent in day 2 and day 3 forecasts make it impossible to accurately forecast extreme ozone events more than one day in advance.

Nighttime Transport

The mode of operation for NETPS required accurate forecasts of transport winds overnight and during the following morning and afternoon. For the purposes of NETPS, forecasts products were developed that included constant-altitude low-level wind maps.

The MM5 consistently produced a phenomenon we will call a “sea-breeze low-level jet”, or SBLLJ. This feature, an inland manifestation of the sea breeze, developed as a low-level enhancement of onshore flow during the late afternoon and early evening. Overnight, the jet would advance inland and gradually turn toward the right, remaining strong overnight but dissipating quickly in the morning. The northwestern edge of this feature was often fairly sharp, and the location and orientation of the jet was sensitive to the large-scale wind patterns.

During the first days of NETPS, forecasters were not certain that the SBLLJ being produced by the model was realistic. The horizontal scale was smaller than the existing profiler network. However, after comparing observations from profilers during a variety of days, it seems clear that a SBLLJ does exist, and that its structure and behavior is similar to that produced by the MM5. Indeed, it is probable that the low-level jet observed on August 30 through September 1, 2000, was such an SBLLJ.

To illustrate the SBLLJ, we show a series of 300m wind fields from the model simulation initialized at 0000 UTC August 2, 2005. At 0300 UTC (10 PM CDT August 1), the SBLLJ is visible as an arc of strong winds about 100 mi inland from the Texas Gulf Coast (Fig. 6). The winds are generally directed toward the northwest, with some variations that reflect the orientation of the coastline. The more well-known Great Plains low-level jet appears as an area of strong winds in Kansas, northwestern Oklahoma, northwestern Texas, and eastern New Mexico.

Three hours later (Fig. 7), the SBLLJ has advanced inland and is now 150 mi from the coastline. Also, the winds of the SBLLJ in Texas have veered somewhat and are now directed from the south. Also worth noting are the strong easterly winds in Mississippi, Arkansas, and Louisiana.

By 0900 UTC (4 AM CDT, Fig. 8) the SBLLJ is in central Texas, approaching the Dallas/Fort Worth area, and its winds have veered to become southwesterly. Core wind speeds

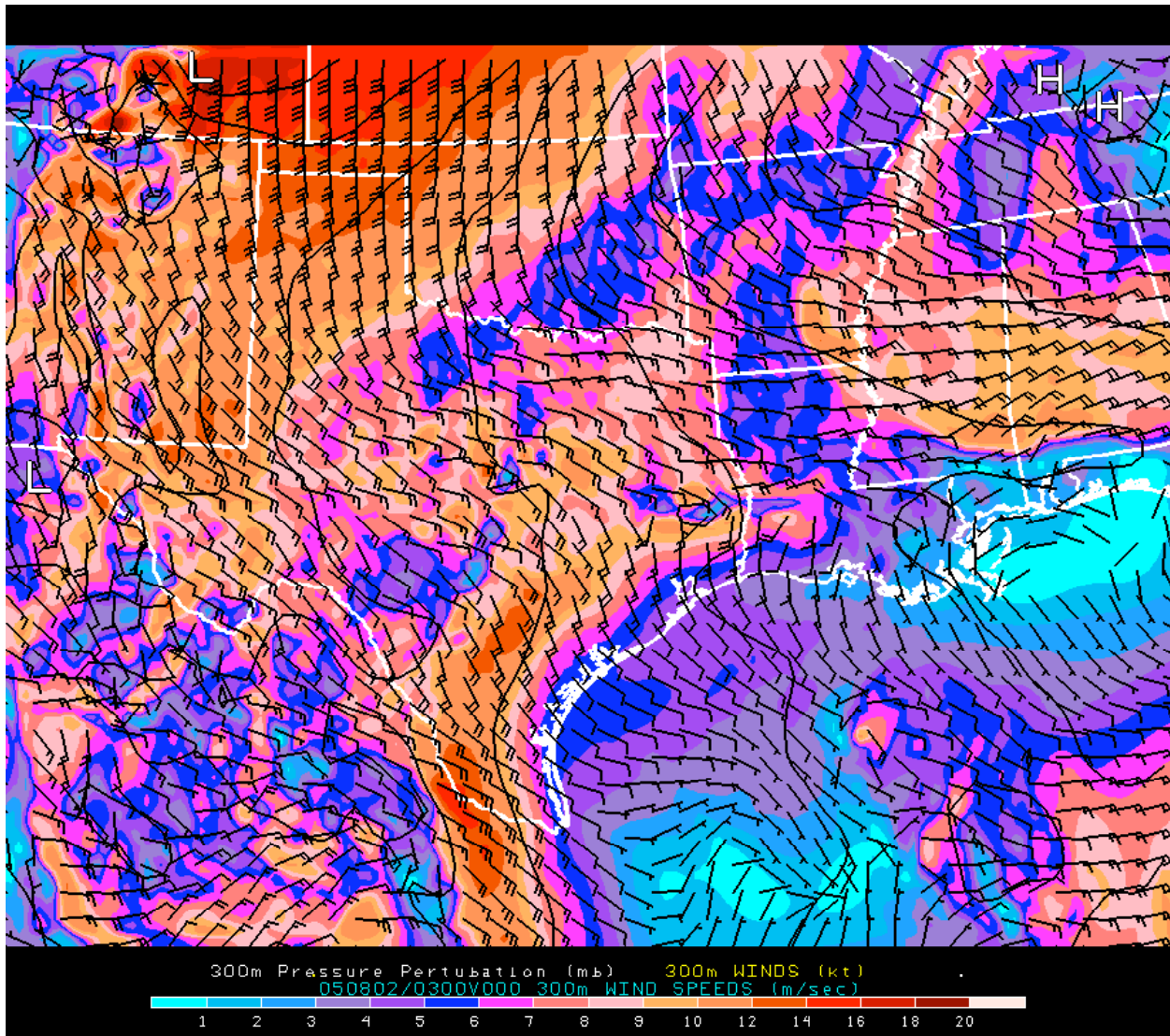


Figure 6: 300 m winds and wind speeds from the 0000 UTC 2 August 2005 MM5 model simulation. The wind speeds are color-coded; the scale (in m/s) is at the bottom of the image. The time depicted is 0300 UTC (the three-hour forecast), or 10 PM CDT August 1.

remain over 10 m/s. Transport of low-level air from Houston to Dallas, which might have been anticipated given the nighttime winds in Fig. 6, has clearly been shut off by the continued veering of the SBLLJ.

By the time of the 12-hour forecast (Fig. 9), the SBLLJ has started to weaken noticeably. The Great Plains low-level jet has also been veering during this period, and has begun to weaken. The transport wind pattern in the ArkLaTex region is complex, to say the least. There is a shear

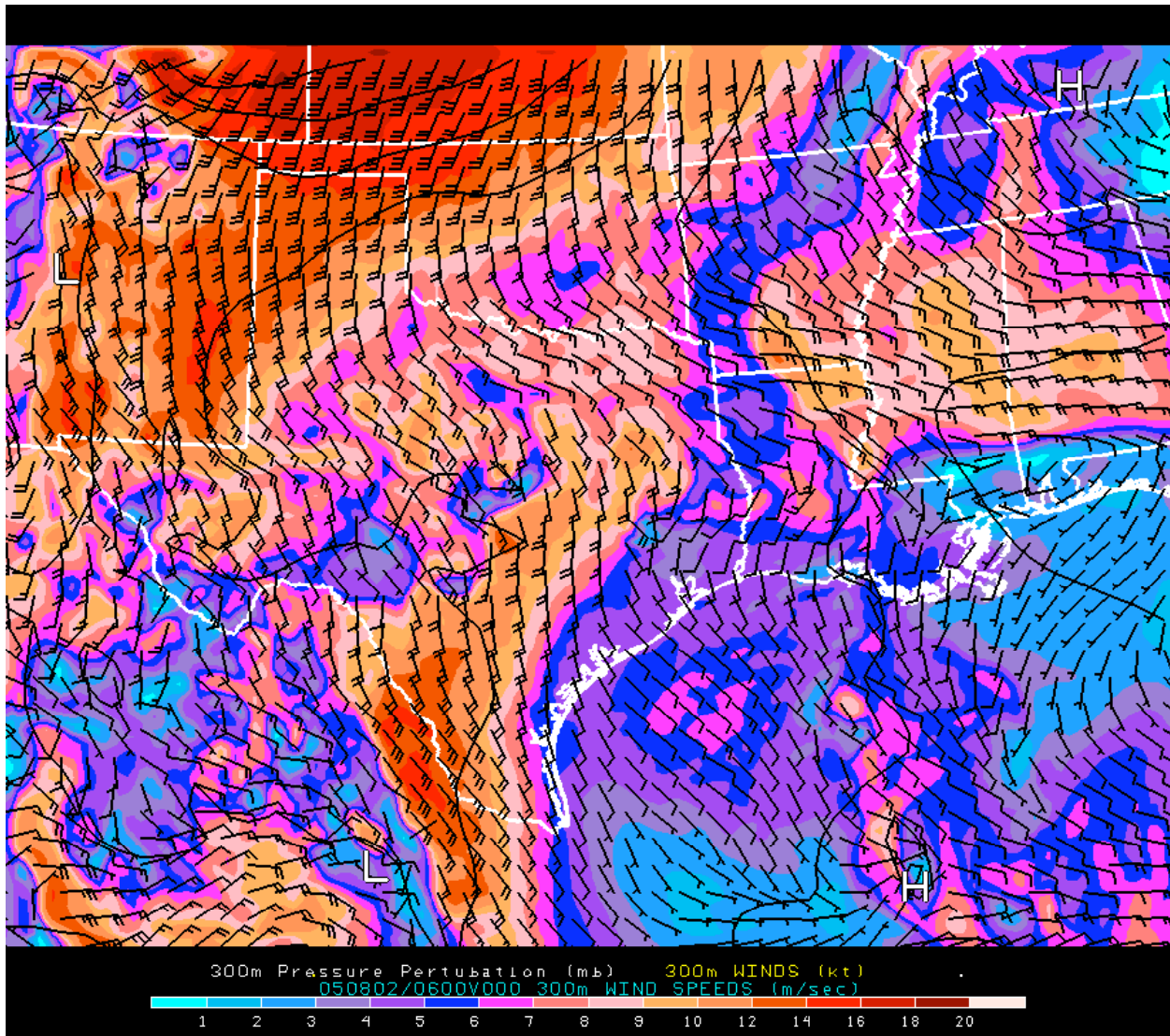


Figure 7: 300 m winds, as in Fig. 6, but for 0600 UTC (1 AM August 2).

line extending along the Red River from the Texas-Oklahoma border into Louisiana. South of the shear line the winds of the remnant SBLIJ are predominantly westerly, while north of the shear line the winds are predominantly southeasterly, a remnant of the wind maximum near the Mississippi River noted earlier.

As the morning progresses, the SBLIJ rapidly vanishes, in its wake leaving weak northwesterly winds (Fig. 10). In the Dallas/Fort Worth area, on this day, the winds have become nearly calm at 10 AM CDT, corresponding to an observed stagnation event and rapid buildup of pollutants.

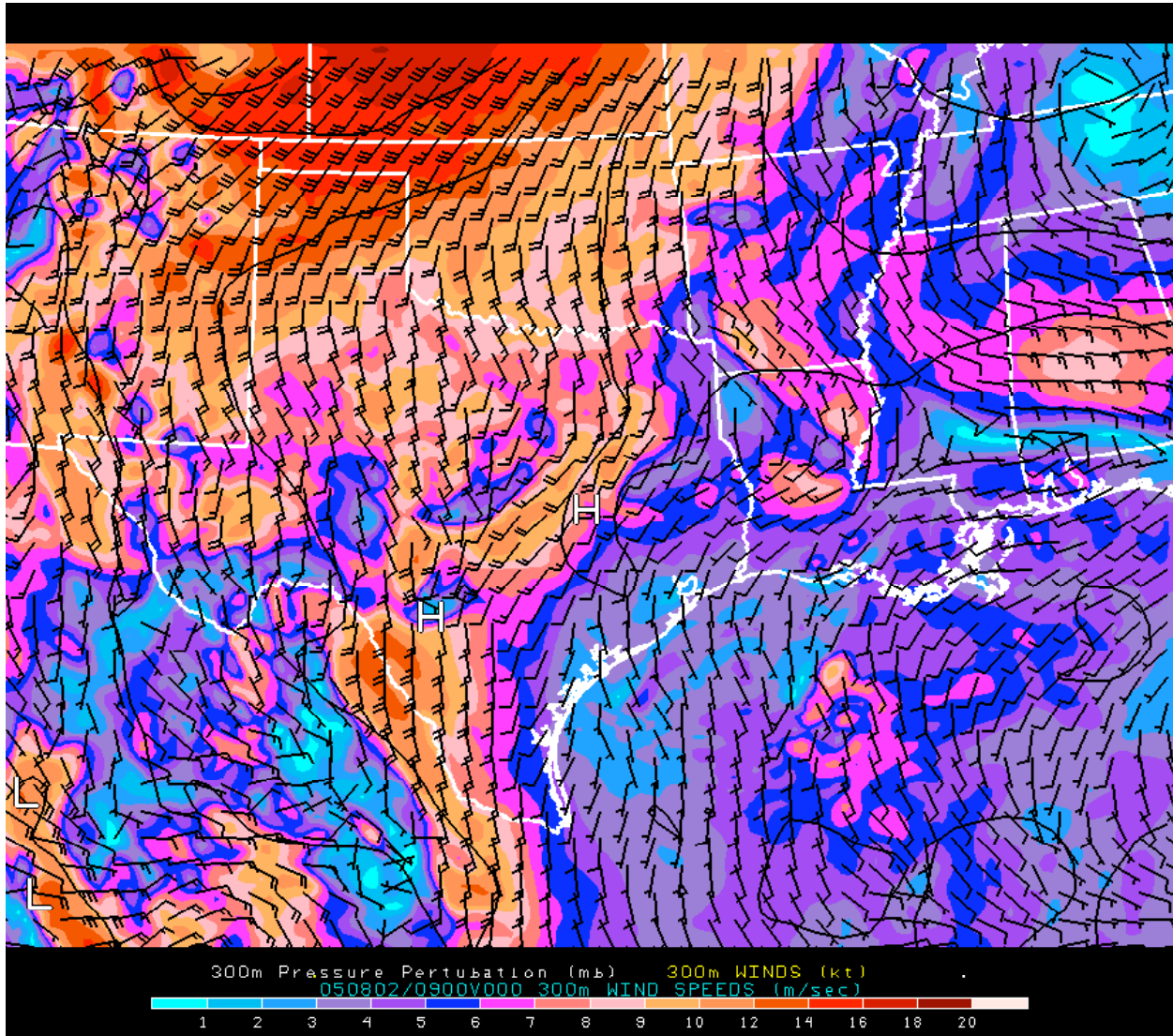


Figure 8: 300 m winds, as in Fig. 6, but for 0900 UTC (4 AM August 2).

By 1 PM CDT (Fig. 11), the northwesterlies have turned to northeasterlies, and the stagnant winds in the Dallas/Fort Worth area have been replaced by easterlies, soon to develop into southeasterlies. There is no longer any evidence of a SBLLJ.

While this basic pattern repeated itself night after night, it was modified considerably by the large-scale wind pattern. When the wind pattern was strong from the southeast, a separate SBLLJ did not form. Instead, a wind maximum, oriented parallel to the coast, would be embedded within the larger-scale low-level jet. An example of this sort of feature is shown in Fig. 12.

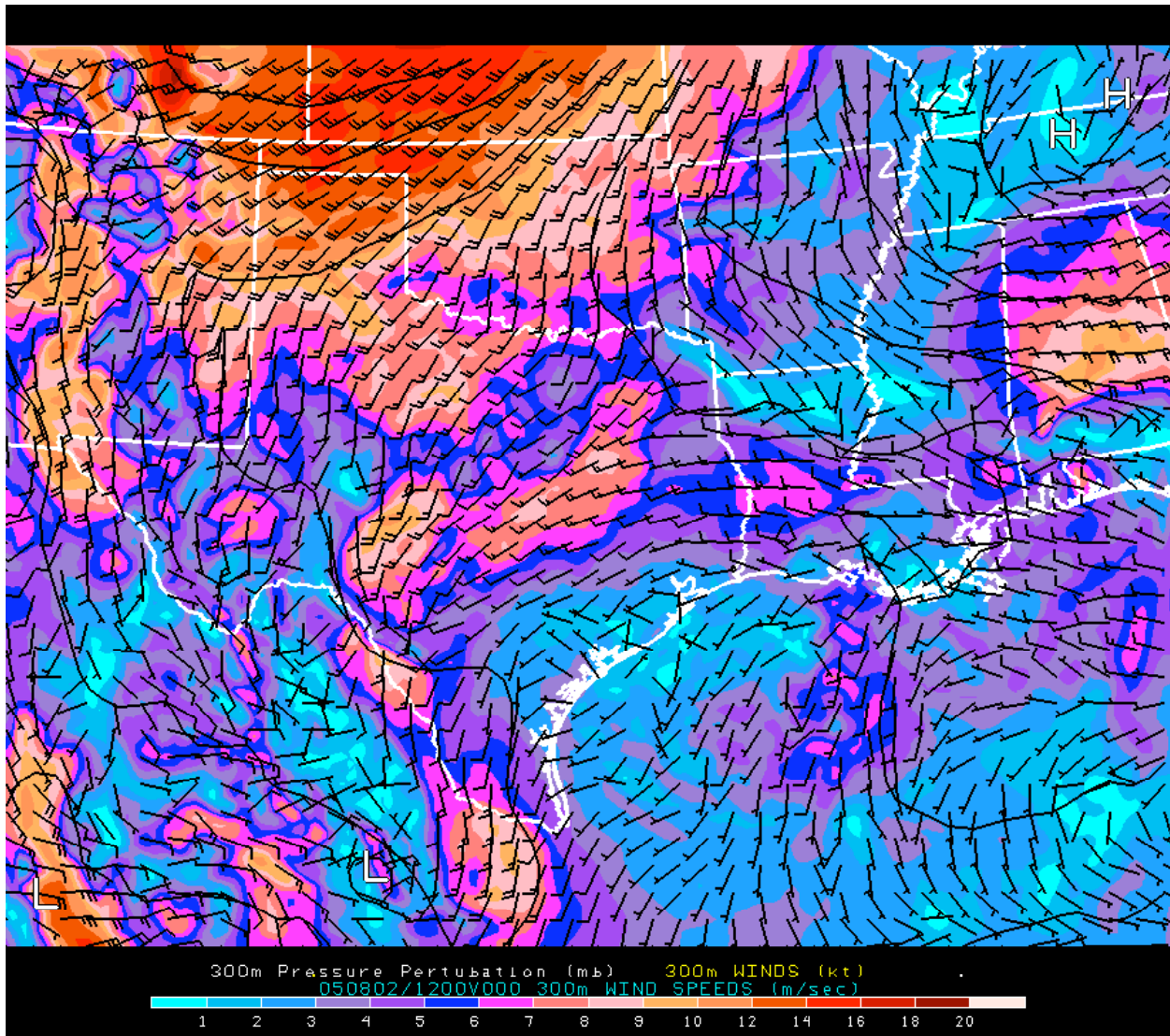


Figure 9: 300 m winds, as in Fig. 6, but for 1200 UTC (7 AM August 2).

Under slightly weaker wind conditions, the SBLLJ remains a distinct entity and can advance all the way to North Texas overnight. Figure 13 shows a forecast from August 21 with strong winds in north-central Texas that originated as a sea breeze surge earlier that evening.

The best observational support for the SBLLJ comes from the profiler network. The SBLLJ in the model forms inland from the coastline, so one would not expect a strong wind maximum at LaPorte. The observations from LaPorte (Fig. 14) confirm this supposition. In this and the following wind profiler figures, two days are depicted. With that much data, it is

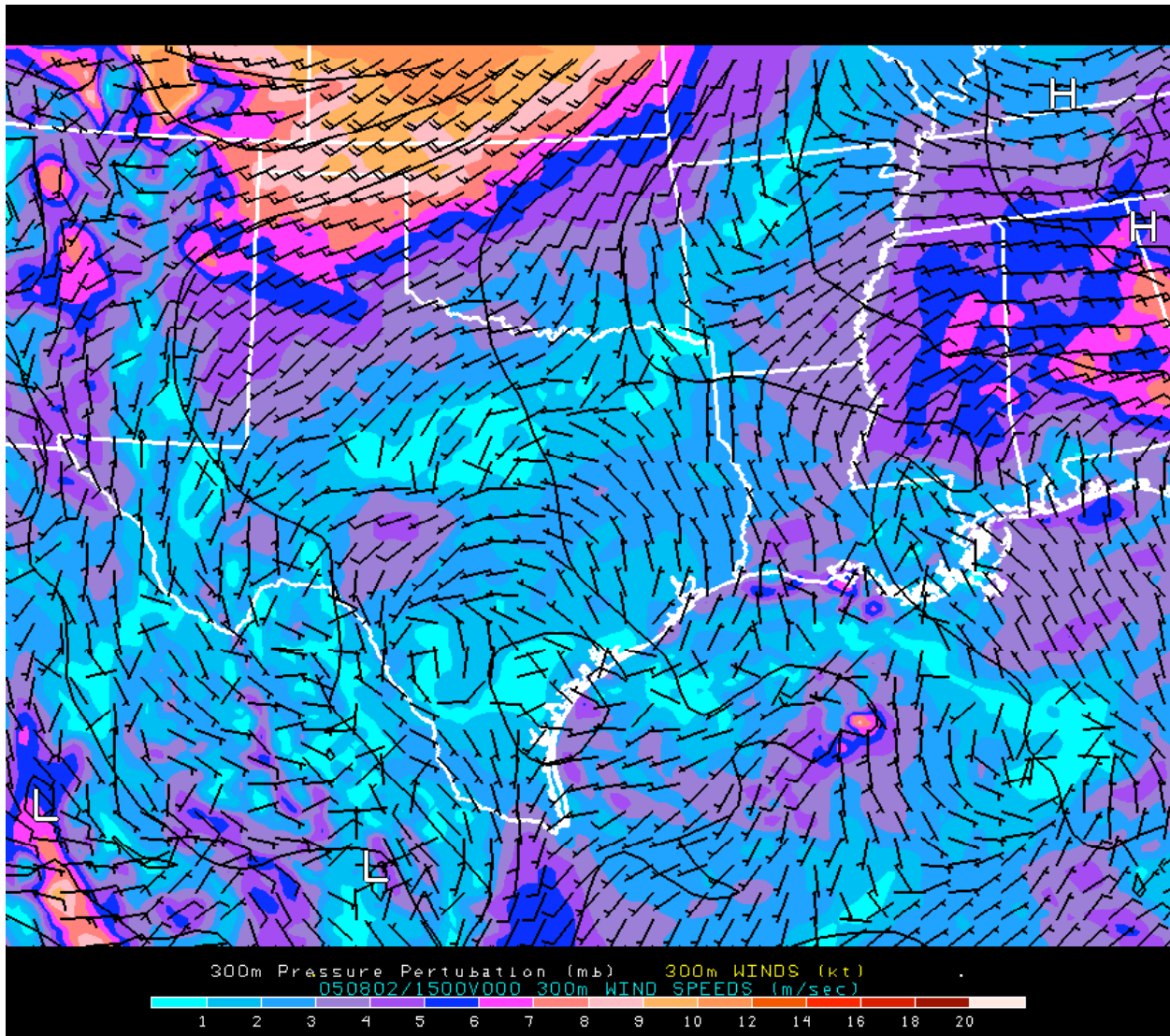


Figure 10: 300 m winds, as in Fig. 6, but for 1500 UTC (10 AM August 2).

difficult to discern individual wind barbs, but the color-coding of the wind barbs clearly shows the pattern of wind speeds. Here it can be seen that on both nights, the winds at LaPorte do not exceed 15 knots. The winds undergo the near-continuous variation of speed and direction expected from the direct effect of the sea breeze, but no strong low-level jet is present.

The next profiler station farther inland is Huntsville. The winds from the Huntsville profiler (Fig. 15) are generally similar to those from the LaPorte profiler, with the exception of the SBLIJ. During the night of August 1 and morning of August 2, the winds below 1000 m

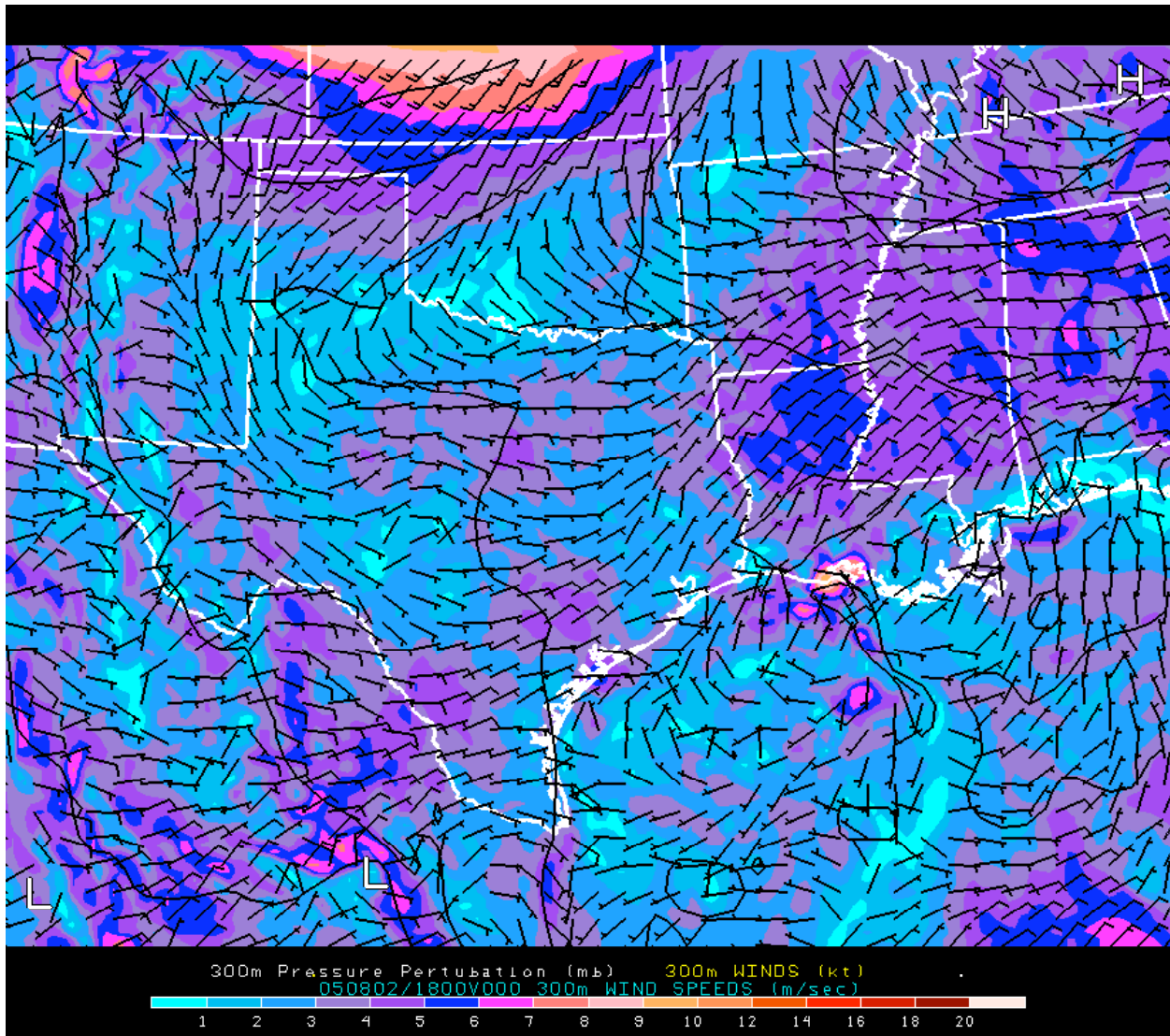


Figure 11: 300 m winds, as in Fig. 6, but for 1800 UTC (1 PM August 2).

become strong from the south and gradually veer before weakening. During the morning hours, the winds become light from the northwest and northeast, consistent with the MM5 forecasted winds. The following night is almost a repeat of the first one. The winds become strong at night, initially from the southeast but then from the south, southwest, and eventually west. The strongest winds are observed in the 300-500 m layer, with wind speeds reaching 20 knots between 0600 UTC and 1000 UTC.

A gap in the profiler network means that the next inland station is Cleburne. The winds from the period are shown in Fig. 16. Unlike Huntsville, no low-level jet is present in Cleburne

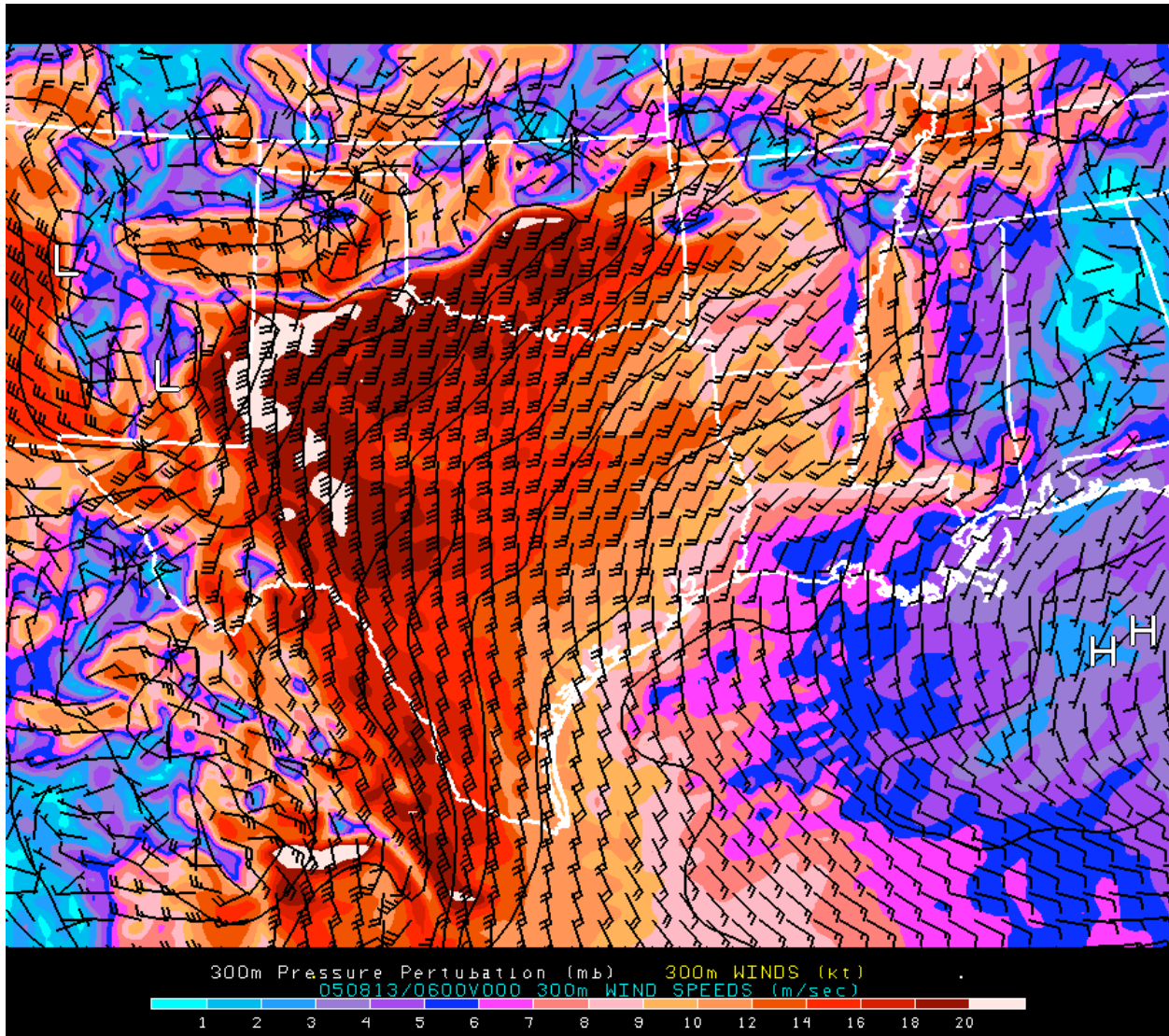


Figure 12: 300 m winds, as in Fig. 6, but for 0600 UTC (1 CDT) August 13, 2005, a 30-hour forecast of the MM5.

on August 2. The winds veer gradually from easterly to southeasterly to southerly to southwesterly overnight, but never exceed 10 knots. Winds become nearly calm between 1500 UTC and 1700 UTC, before strengthening a bit from the southeast.

This wind evolution is very similar to the evolution forecasted for the Dallas/Fort Worth area by the MM5 model. In the model forecast, the SBLIJ never reached as far north as the Dallas/Fort Worth area, so the winds remained light and gradually veered overnight. During the following day, in the model, winds stagnated around 1500 UTC (10 AM CDT). The primary

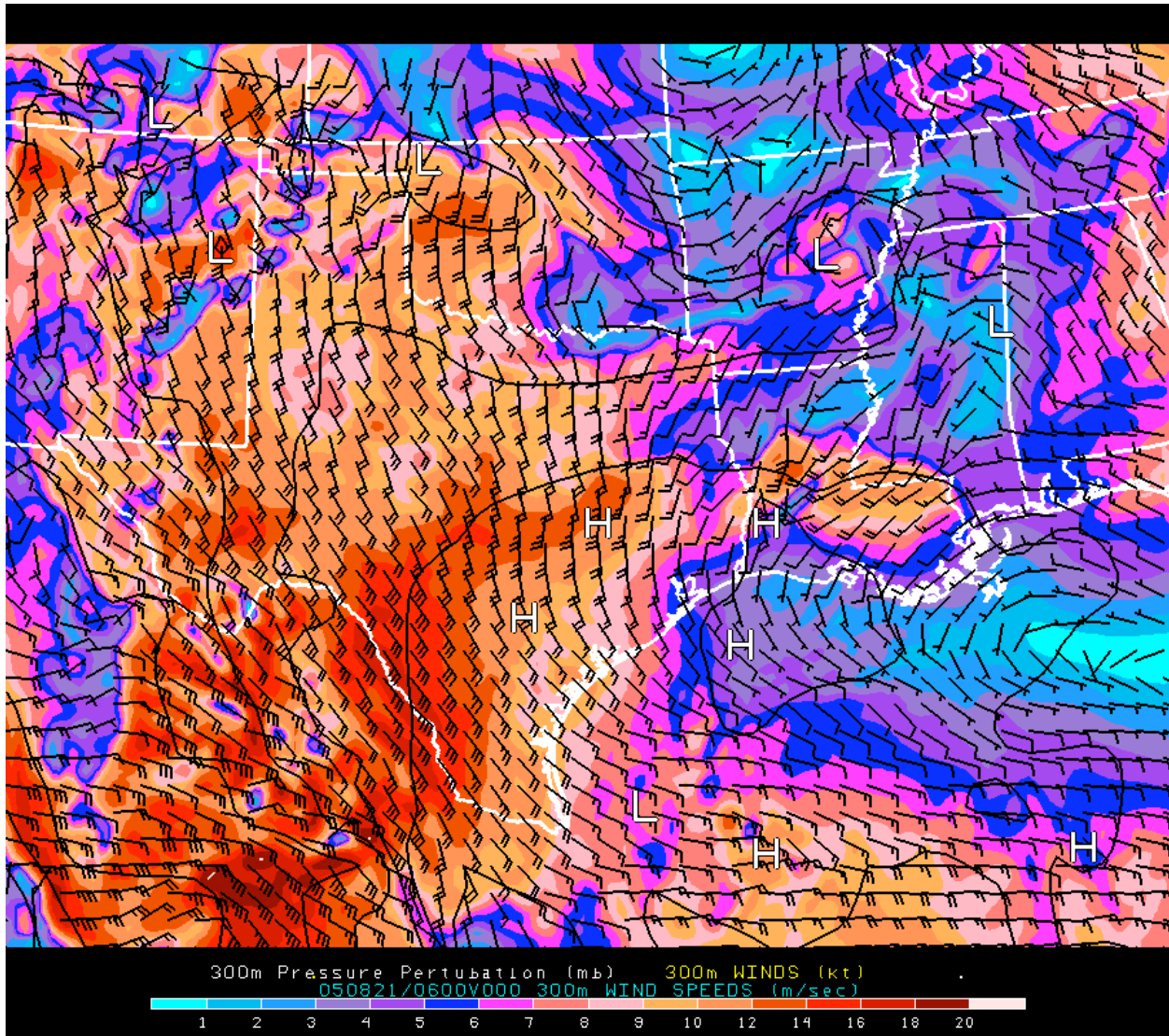


Figure 13: 300 m winds, as in Fig. 6, but for 0600 UTC (1 CDT) August 21, 2005, a 6-hour forecast of the MM5.

difference with the MM5 compared to observations is that the winds were from the southeast rather than the east in the early afternoon.

The following night, consistent with the stronger winds observed in Huntsville, the SBLIJ does appear to reach Cleburne. Between 0700 and 0900 UTC the winds are from the south at speeds approaching 20 knots. The rapid decrease of wind speed during the morning is remarkable: by 1500 UTC the winds are less than 5 knots as the SBLIJ has dissipated.

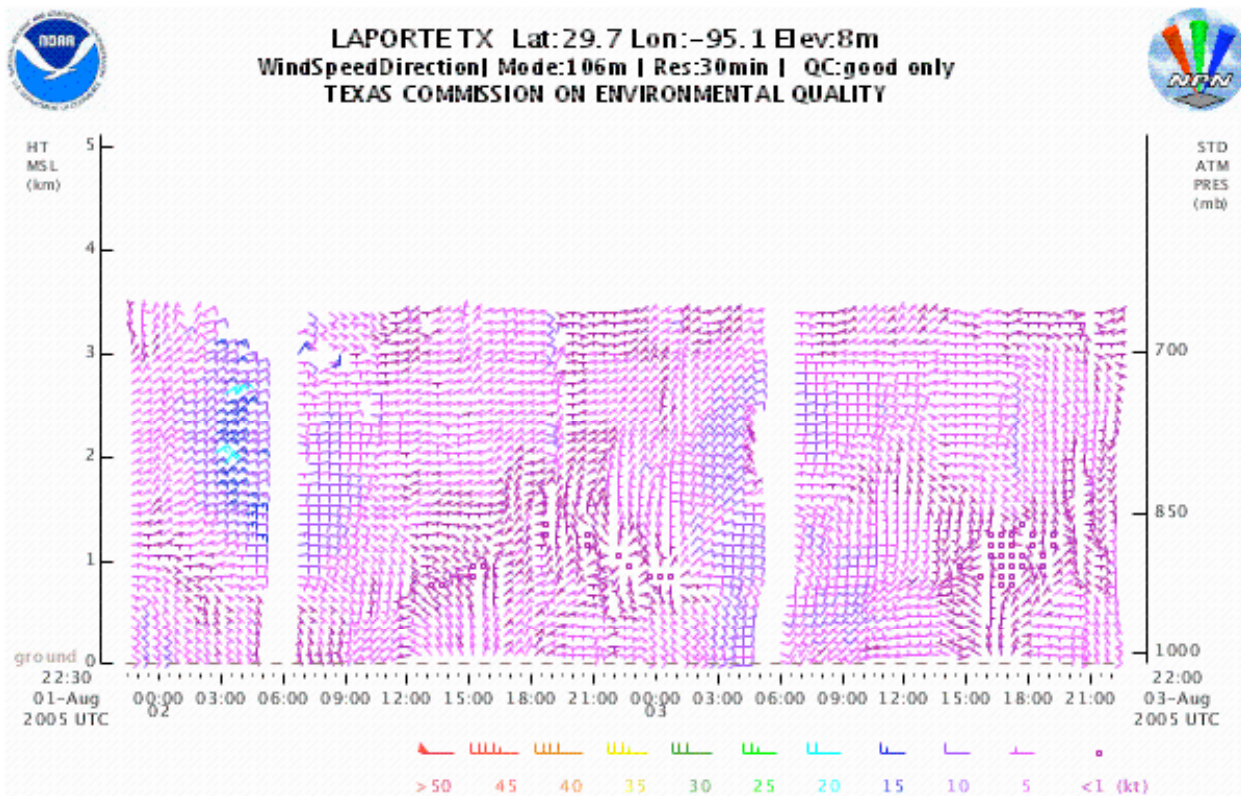


Figure 14: Observed winds at LaPorte profiler, as in Fig. 3, but for August 2-3.

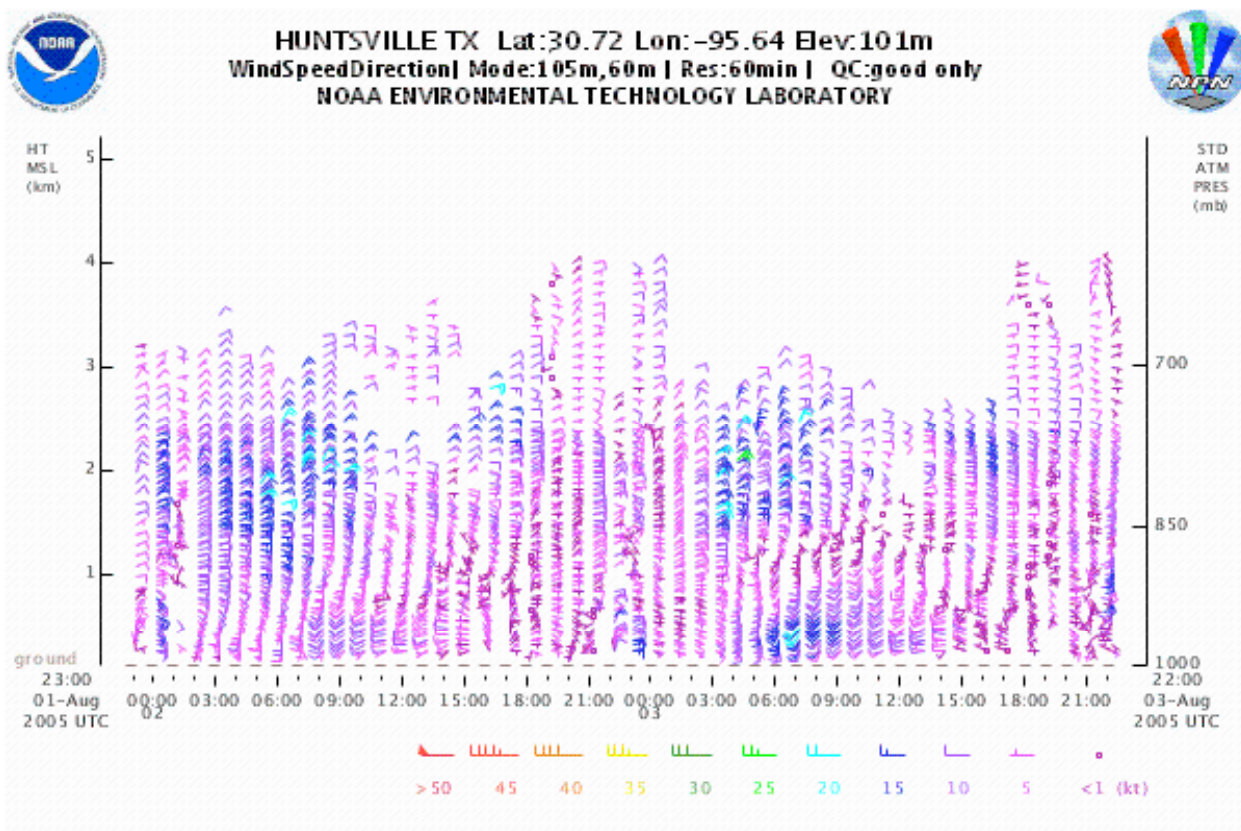


Figure 15: Observed winds at Huntsville profiler, August 2-3.

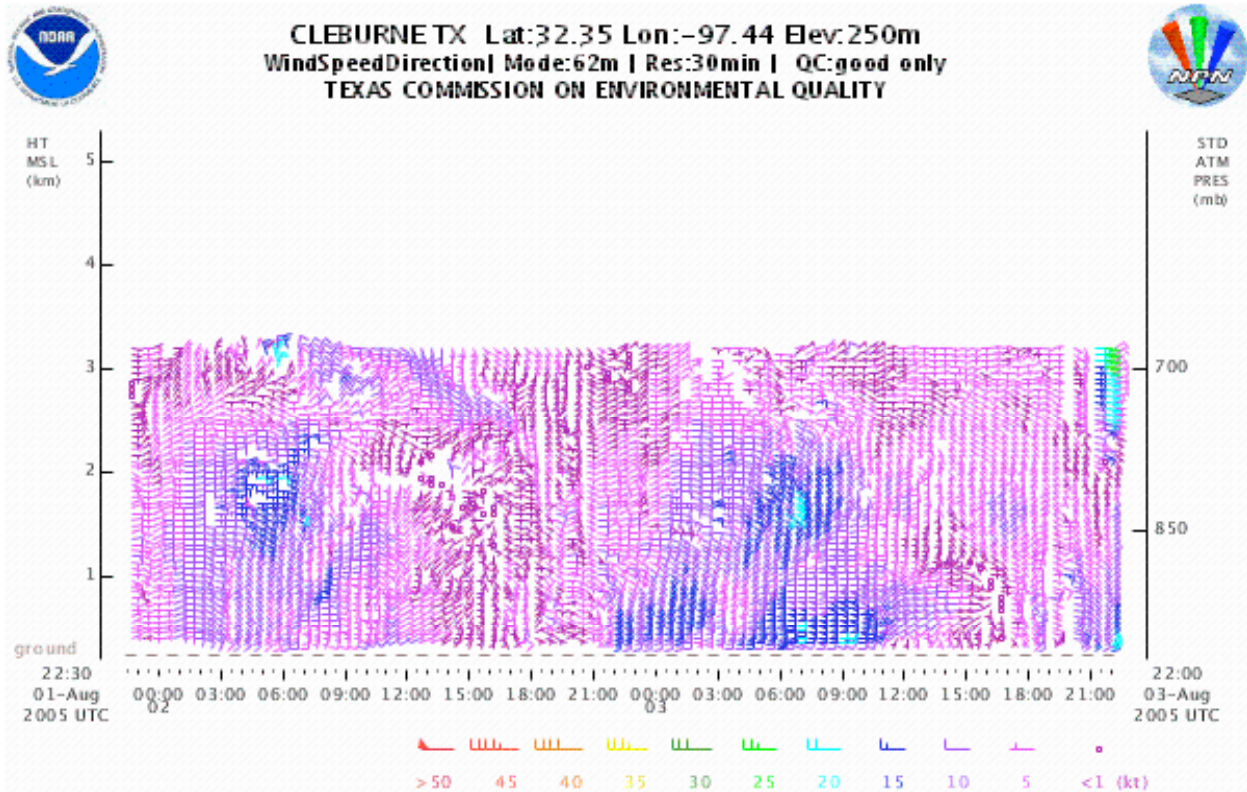


Figure 16: Observed winds at Cleburne profiler, August 2-3.

It is of interest to note that at Longview (not shown), the profiler detected the strong low-level easterlies on August 2 that were forecasted to be in Louisiana and Arkansas. This is an example of the forecast model producing the right phenomena but not quite getting them in the right place.

While heretofore undocumented observationally, the SLLJ appears to be a straightforward physical phenomenon. The land-sea temperature difference causes a landward acceleration of the winds. As the pressure gradient persists around nightfall, the onset of stable stratification causes the winds, no longer retarded by surface friction, to accelerate inland more strongly. During the night, as the coastal pressure gradient vanishes and the winds advance inland, they rotate clockwise under the influence of the Coriolis force, much as the winds rotate along the coast. But because the winds were so strong initially, the SLLJ winds remain strong as they rotate. At their leading edge, weaker winds are overtaken by stronger winds, leading to a sharp wind speed and air mass gradient there. Meanwhile, at the trailing edge, the same sort of effect weakens the gradient and makes the southern edge of the SLLJ gradual and indistinct.

The existence of the SBLLJ makes the weather conditions sought in the NETPS (light, steady nighttime southeasterly flow) unlikely to actually occur. While the EDAS analyses (and any trajectories created from them using HySplit) hint at this phenomenon, they grossly underestimate the magnitude of the SBLLJ and the resulting nighttime wind rotation, seen both in the enhanced profiler network and the MM5 forecasts. Also, transport from Houston to Dallas will not be easily separated from the specific wind conditions the following day. It is not clear whether Houston-Dallas transport, followed by high ozone in Dallas, is a common sequence of events, but it is clear that any attempt to model transport from Houston to Dallas must have sufficient vertical resolution to properly simulate both the sea breeze itself and the resulting SBLLJ.

Precipitation

The model's forecasts of precipitation were not as reliable as its forecasts of winds and temperatures. In part, this is to be expected: summertime convection is inherently unpredictable. For forecasting precipitation during daytime in Houston and even Dallas, morning observations of offshore convection and GPS precipitable water were much more useful.

Despite the low expectations for the cumulus parameterization, the model still performed below expectations. An example of a model prediction of accumulated precipitation is shown in Fig. 17. This forecast took place during an episode in which there was considerable precipitation in central Texas for several days.

The boundaries of the inner domain are obvious. On the 12 km domain, the model forecasts widespread but light precipitation. On the inner domain, the spatial coverage of the precipitation is much less but the precipitation intensity is much greater.

This sort of error is well known in modeling and is caused by the cumulus parameterization producing precipitation under circumstances in which the explicit high-resolution nest does not. The parameterization scheme makes the atmosphere too stable, so while instability builds up, little precipitation is forecasted. Finally, well inside the inner nest, convection finally develops and is too intense.

Errors in the forecasts of convection will have a direct impact on temperatures and winds in the vicinity of the convection. Because precipitation processes affect deep tropospheric

temperatures and pressures, a systematic error of precipitation distribution will lead to systematic wind errors on a large scale too.

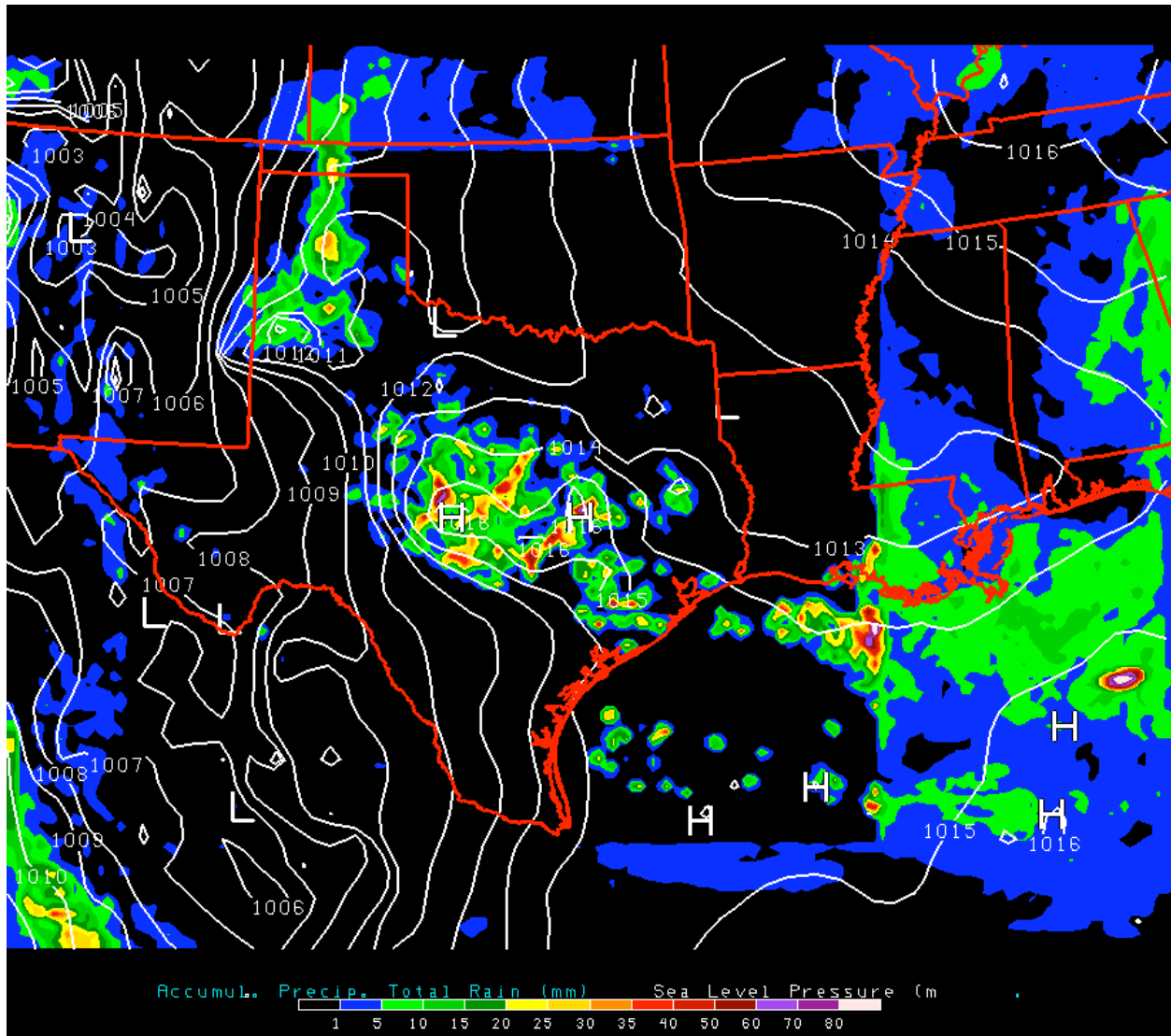


Figure 17: Accumulated precipitation (mm) in a 24-hour forecast using the Grell cumulus parameterization scheme on the 36 km and 12 km grids and no parameterization on the 4 km grid.

While it would require an extensive verification effort to ascertain the correct pattern of precipitation and quantitatively determine the accuracy of this forecast, we know even without verifying that a systematic difference in the behavior of precipitation across the boundary of the 4 km inner domain is nonphysical. To investigate whether a different choice of cumulus parameterization scheme would show less of an effect across the 4 km boundary and would

perform better overall, a series of 16 experiments were conducted. Some produced the opposite effect: more precipitation outside the 4 km domain than inside it. Some exhibited no boundary effect at all. Of the latter class, the precipitation distribution that most closely matched the observed precipitation pattern was the model run performed with the Kain-Fritsch 2 scheme on all three nests (Fig. 18).

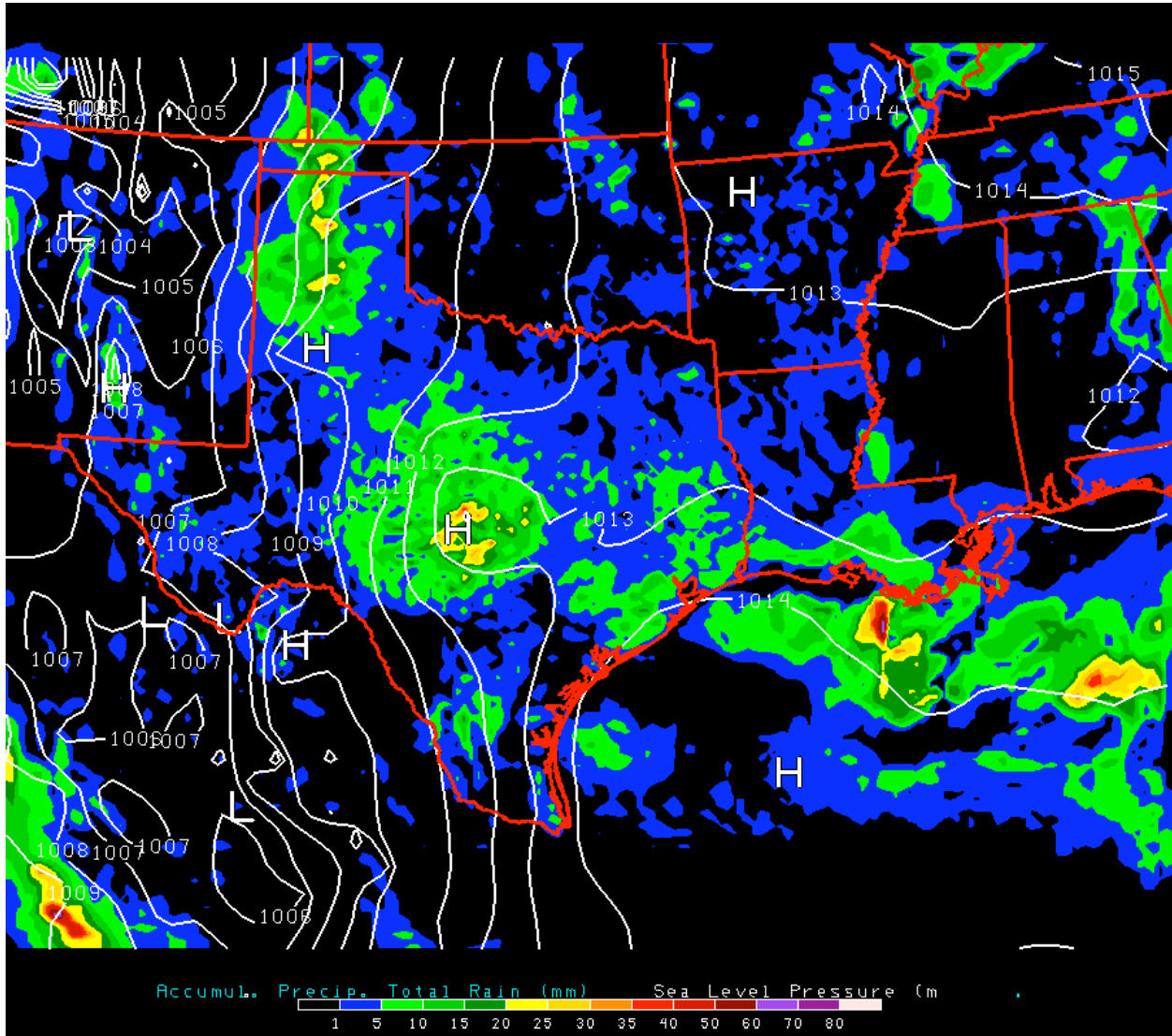


Figure 18: Accumulated precipitation, as in Fig. 17, but for a model run utilizing the Kain-Fritsch 2 cumulus parameterization scheme on all three grids.

Because of its superior performance, we plan to change to the better-performing cumulus parameterization configuration prior to the 2006 field operations, and we will use this configuration for retrospective modeling as well.

Summary of Part III

The MM5 performed adequately in summer 2005, providing valuable support for meteorological and ozone forecasting and field operations. The model even revealed the existence of an important intrastate transport phenomenon heretofore undocumented: the sea-breeze low-level jet, or SBLLJ. The SBLLJ is a low-level wind surge that forms just inland from the coastline and advances inland, eventually becoming a shore-parallel wind maximum just before sunrise, after which it dissipates. The SBLLJ appears to be caused by a combination of the sea breeze pressure gradient itself and nighttime frictional decoupling, and its change in wind direction appears to be caused by the Coriolis force. The SBLLJ will greatly modulate intrastate and interstate transport during light wind conditions when initial ozone and ozone precursor concentrations are likely to be highest.